Cell, Vol. 84, 61–71, January 12, 1996, Copyright ©1996 by Cell Press

Cytokinesis in the Arabidopsis Embryo Involves the Syntaxin-Related KNOLLE Gene Product

Wolfgang Lukowitz,* Ulrike Mayer,* and Gerd Jürgens*
Institut für Genetik und Mikrobiologie
Lehrstuhl für Genetik
Universität München
D-80638 München
Federal Republic of Germany

Summary

The embryo of the flowering plant Arabidopsis develops by a regular pattern of cell divisions and cell shape changes. Mutations in the *KNOLLE* (*KN*) gene affect the rate and plane of cell divisions as well as cell morphology, resulting in mutant seedlings with a disturbed radial organization of tissue layers. At the cellular level, mutant embryos are characterized by incomplete cross walls and enlarged cells with polyploid nuclei. The *KN* gene was isolated by positional cloning. The predicted KN protein has similarity to syntaxins, a protein family involved in vesicular trafficking. During embryogenesis, *KN* transcripts are detected in patches of single cells or small cell groups. Our results suggest a function for *KN* in cytokinesis.

Introduction

Cytokinesis partitions the cytoplasm of a dividing cell following the separation of the daughter chromosomes. This basic cellular process occurs in a variety of ways in eukaryotes (for recent review see Fishkind and Wang, 1995). Plant cells are unique in that they initiate cytokinesis in the center of the division plane: Golgi-derived vesicles accumulate and fuse to form an immature cross wall, the cell plate, which then grows toward the parental wall (Gunning, 1982). Although the physical separation of daughter cells starts in the center, the plane of cell division is marked well before the onset of cytokinesis by a transient structure forming at the periphery, the cortical preprophase band of microtubules (Wick, 1991).

Little is known about the mechanism of cell plate formation. Between the separating anaphase chromosomes, two groups of microtubules interdigitate with their plus ends at the plane of division, forming the so-called phragmoplast (Lambert, 1993). Polypeptides with microtubule-translocating activity that have been isolated from phragmoplasts of tobacco cells may be involved in transporting microtubule-associated membrane vesicles to the site of cell plate formation (Asada and Shibaoka, 1994). How vesicle fusion is brought about at the site of cell plate formation is not known. However, studies in budding yeast and animal nerve cells indicate that the molecular machinery of vesicular trafficking is highly conserved (Bennett and Scheller, 1993). A family of membrane-anchored proteins, the syntaxins, have been implicated in directing vesicle transport, with specific syntaxins mediating fusion events in different pathways.

Embryogenesis of the flowering plant Arabidopsis involves regular patterns of cell divisions and cell shape changes (Mansfield and Briarty, 1991; Jürgens and Mayer, 1994). Oriented cell divisions are associated with the formation and development of tissue primordia. An outer layer of epidermis precursor cells originates from tangential cell divisions within the 8-cell embryo. Slightly later, the inner cells produce, again by oriented divisions, the centrally located vascular precursor cells and the surrounding ground tissue. As a result, these major types of plant tissues are arranged in concentric layers that constitute the radial pattern of the seedling. Mutations disrupting cell divisions or cell morphology might thus be expected to result in abnormal seedlings. Such mutations would provide a means of analyzing cellular processes during plant embryo development.

A systematic screen for mutations affecting the body organization of the Arabidopsis seedling led to the identification of the *KNOLLE* (*KN*) gene (Mayer et al., 1991). Mutant *knolle* (*kn*) seedlings lack a well-formed epidermis layer, apparently owing to abnormal cell divisions and cell enlargement during embryogenesis. To determine the cellular basis of the radial pattern defect, we have analyzed the development of *kn* embryos and characterized the *KN* gene molecularly. Our results suggest that the *KN* gene encodes a novel syntaxin-related protein that is involved in cytokinesis.

Results

The *KN* gene has been identified in a genetic screen for mutations affecting the body organization of the Arabidopsis seedling (Mayer et al., 1991). Three alleles, one ethyl methanesulfonate (EMS) induced and two X-ray induced, give essentially the same mutant phenotype, which, as shown below, is likely caused by complete inactivation of the gene. The proportion of mutant embryos among the progeny of heterozygous plants is about 25%, indicating that *KN* is not required for normal development of the haploid gametophytic generation. Depending on culture conditions, a variable number of mutant seeds containing mature embryos does not germinate. The phenotype of *kn* seedlings ranges from white, tuber-shaped to green elongated individuals (Figures 1a and 1b). *kn* seedlings lack functional meristems and, at varying times after seed germination, show patches of necrotic tissue and eventually die.

Radial Pattern Defects in *kn* Seedlings

Wild-type seedlings display a characteristic body organization, consisting of an apical–basal pattern along the body axis and a radial pattern perpendicular to that axis. Main elements of the apical–basal pattern are two cotyledons, a hypocotyl, and a root. All *kn* seedlings have clearly distinguishable although malformed cotyledons and a shortened root (Figure 1b). In weakly affected seedlings, the cotyledons are green and the root has

* Present address: Lehrstuhl für Entwicklungsgenetik, Universität Tübingen, Spemannstrasse 37-39, D-72076, Tübingen, Federal Republic of Germany.

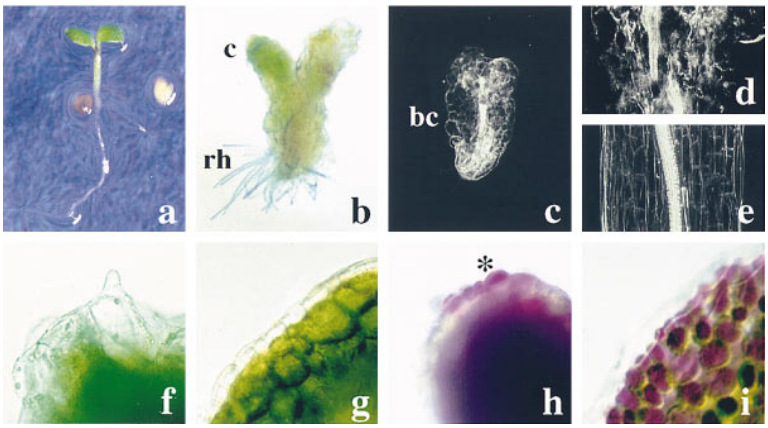

Figure 1. Phenotype of *kn* Seedlings

(a) Wild-type (left) and *kn* seedling (right).

(b) *kn* seedling stained with methylene blue (0.05%). Cotyledons (c) and root hairs (rh) are indicated.

(c) *kn* seedling (dark-field optics); bc, bloated cells.

(d–e) Vascular strands in the hypocotyl of *kn* (d) and wild-type (e) seedlings (dark field optics).

(f–g) Distribution of chlorophyll in cotyledons of *kn* (f) and wild type (g).

(h–i) Distribution of anthocyanin in cotyledons of *kn fus* (h) and *fus* (i) mutants; asterisk indicates surface cell containing anthocyanin.

All panels except (a) are shown to scale.

well-formed root hairs. The hypocotyl is represented by an abnormally widened and shortened stem-like segment that separates the root from the cotyledons. As in wild type, the root, but not the hypocotyl, shows a characteristic birefringence in dark-field optics (Figure 1c). Thus, the major elements of the apical–basal pattern appear to be present in *kn* seedlings.

The radial pattern of wild-type seedlings is a regular concentric arrangement of tissue layers. Three major types of tissue are usually distinguished: centrally located vasculature, ground tissue, and epidermis at the surface. In *kn* seedlings, both shape and arrangement of cells is abnormal, making it difficult to identify organized layers of tissue. For example, *kn* seedlings have irregularly arranged bloated cells at their surface, which do not morphologically resemble a wild-type epidermis (Figures 1b and 1c). However, *kn* seedlings show some differentiation of all major tissue types. Strands or lumps of xylem cells with spiral wall thickenings are found in the hypocotyl of mutant seedlings (Figures 1c–1e). As in wild type, mesophyll cells with a high density of chloroplasts form the ground tissue in the cotyledons of *kn* seedlings (Figures 1f and 1g). The surface cells of *kn* cotyledons contain a few chloroplasts and thus are similar to wild-type epidermal cells, which rarely differentiate chloroplasts. To confirm the identity of the surface cells in *kn* seedlings, we examined the distribution of anthocyanin in a *fusca* (*fus*) mutant background: *fus* mutations specifically cause the accumulation of anthocyanin (purple pigment) in the vacuoles of subepidermal, but not epidermal, cells (Miséra et al., 1994). In *kn fus* double mutant seedlings, most of the outer cells are transparent, but a minority accumulates high levels of anthocyanin (Figures 1h and 1i). Thus, while *kn* seedlings can differentiate features characteristic for each of the three major tissue types, the morphology and arrangement of their cells is disturbed.

Development of *kn* Embryos

To determine the origin of the *kn* seedling phenotype, we compared the development of *kn* embryos with wild-type embryogenesis (Figure 2). *kn* mutants deviate from normal development before the 8-cell stage. In *kn* embryos, newly formed cross walls are misoriented (compare Figures 2a and 2b with 2e and 2f). At the 8-cell stage, tangential cell divisions normally separate a group of inner cells from the outer layer of epidermal precursor cells (Figures 2f and 2g). In *kn* embryos, these oriented cell divisions do not occur, and no distinct inner

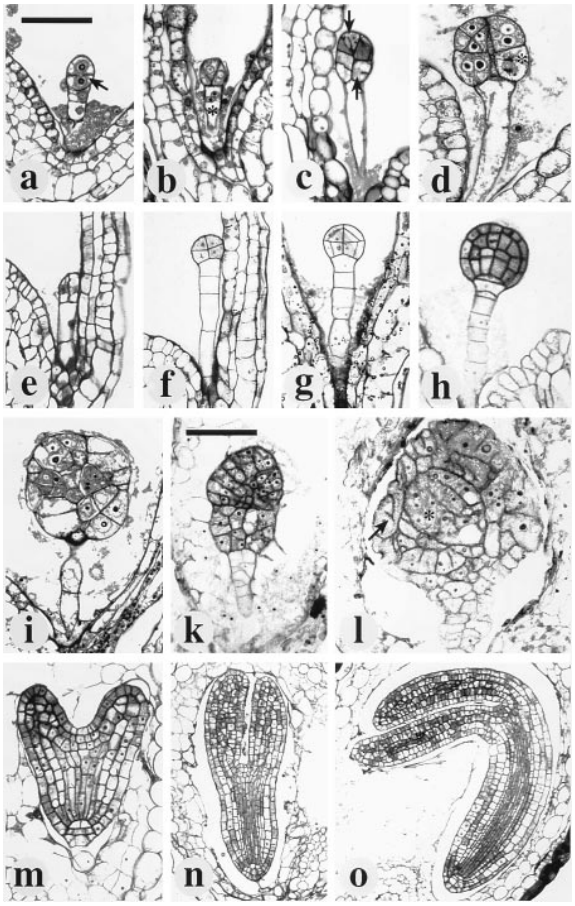

Figure 2. Development of *kn* Embryos

Plastic sections of *kn* (a–d and i–l) and wild-type embryos (e–h and m–o). Developmental stages are as follows: (a) and (e), 4-cell stage; (b) and (f), 8-cell stage; (c) and (g), dermatogen; (d) and (h), globular; (i) and (m), heart; (k) and (n), torpedo; (l) and (o), bent cotyledon. Asterisks indicate mitotic figures and multinucleate cells; arrows indicate incomplete cross walls.

Scale bar is 50 μm in (a)–(i) and (m) and 100 μm in (k), (l), (n), and (o).

or outer cells are formed (Figures 2b and 2c). Subsequent cell divisions appear random and seem to occur more slowly, such that the globular-stage embryo has fewer but larger cells as compared with wild type (compare Figure 2d with Figure 2h). The extraembryonic suspensor, which supports the embryo, also consists of fewer cells, in most cases one or two cells (Figures 2b–2d) in comparison with five to eight cells in the wild-type embryo (Figures 2f–2h). From the heart stage on, primordia of seedling structures are morphologically distinguishable in the wild-type embryo. For example, elongated cells in the center of the embryo will eventually give rise to the vascular strands of the hypocotyl (Figures 2m–2o). In *kn* embryos, however, primordia of seedling structures cannot be recognized by cell shape or arrangement at any time (Figures 2i–2k). Mutant embryos are irregularly shaped, displaying both enlarged and small cells seemingly at random. Mature *kn* embryos have fewer cells in comparison with wild type. Thus, mutations in the *KN* gene disrupt the regular pattern of Arabidopsis embryogenesis by altering the rate and plane of cell division as well as cell morphology.

Cellular Defects in *kn* Embryos

kn embryos display a characteristic cellular phenotype at all stages of development. The cells often contain more than one nucleus, and occasionally the nuclei appear to be closely associated (examples are indicated by asterisks in Figures 2b and 2l). In tissue sections, a large number of incomplete cell walls can be observed. The cell wall defects are variable, ranging from fragmentary, sometimes T-shaped cross walls to walls with small gaps (examples are indicated by arrows in Figures 2a, 2c, and 2l). Gaps are often confined to one section in a consecutive series (data not shown), making it difficult to determine whether all or only some cross walls are defective. In plant cell division, the newly formed cross wall is thought to be derived from a cell plate that typically forms in the center of the plane of cell division and grows toward the periphery to fuse with the parental cell wall (for review see Wick, 1991). In *kn* embryos, cross wall fragments are usually found attached to the parental cell wall, as if they were produced by growth from the periphery toward the center. Electron microscopic analysis is consistent with these observations and also reveals that in cells with fragmentary cross walls adjacent nuclei are not separated by plasma membranes (Figures 3a and 3b). These features indicate that cytokinesis is affected in *kn* embryos.

Mitotic figures are frequently observed in sections of *kn* embryos (e.g., Figure 2d), and many nuclei appear enlarged. Nuclear stainings of squashed mutant embryos show that most nuclei contain an increased number of chromosomes (Figures 3c and 3d). Up to 80 chromosomes, or eight times the diploid complement, were counted in individual nuclei (data not shown). Thus, *kn* mutations also result in endomitotic cycles that appear to correlate with cell enlargement.

Isolation of the *KN* Gene by Positional Cloning

To determine the primary function of the KN protein, we have isolated the *KN* gene by molecular mapping and

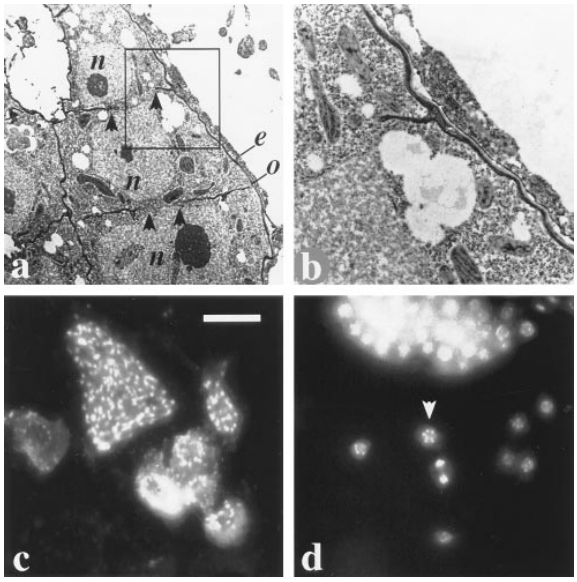

Figure 3. Cellular Defects in *kn* Embryos

(a and b) Electron micrographs; (a) is an overview. Outer cell wall (o), endosperm (e), and nuclei (n) are indicated; arrowheads highlight incomplete cross walls. (b) is a magnification of the region boxed in (a), showing a cross wall fragment attached to the outer cell wall. No plasma membrane can be recognized between the two nuclei (see [a]).

(c and d) Nuclear staining of *kn* (c) and wild-type (d) cells; *kn* nuclei show a variably increased number of heterochromatic dots compared with wild type; arrowhead in (d) points out seven dots in a wild-type nucleus.

Box width in (a) is 5 μm; (c) and (d) are shown to scale (bar is 20 μm).

chromosome walking (Figure 4). The *KN* gene maps to a genetic interval of chromosome 1 defined by the morphological markers *an* and *dis1* (data not shown). Four restriction fragment length polymorphism (RFLP) markers (*m488*, *m322*, *m219*, and *g5957*; Hauge et al., 1993) were found to be closely linked, converted to polymerase chain reaction (PCR) markers (codominant amplified polymorphic sequences, or CAPS), and used to analyze a segregating population representing about 2700 meiotic events. The *KN* gene was mapped to an interval of less than 1 cM (CAPS *5957–322* interval), for which 18 recombinants could be used in monitoring a chromosome walk (Figure 4a).

Yeast artificial chromosome (YAC) clones that had been anchored to *g5957* and *m322* were aligned to establish a contig of cloned genomic DNA (Figure 4b; *EG11A5*, Hwang et al., 1991; *EG12E7*, Whitelam et al., 1993; *yUP* clones, P. Dunn, E. Matallana, and J. Ecker, personal communication). To confirm the alignment, we mapped two polymorphic YAC ends relative to the *KN* gene. The YAC clone *yUP7F4* is about 250 kb long and was found to cover ten recombination events, suggesting a mapping resolution of about 25 kb. A similar value was expected for the physical distance between the *KN* gene and the nearest marker, CAPS *5957* (Figures 4a and 4b), and the *5957* PCR product was thus used for initiating a chromosome walk with phage and cosmid clones (Figure 4c). The left-end fragment of one of the

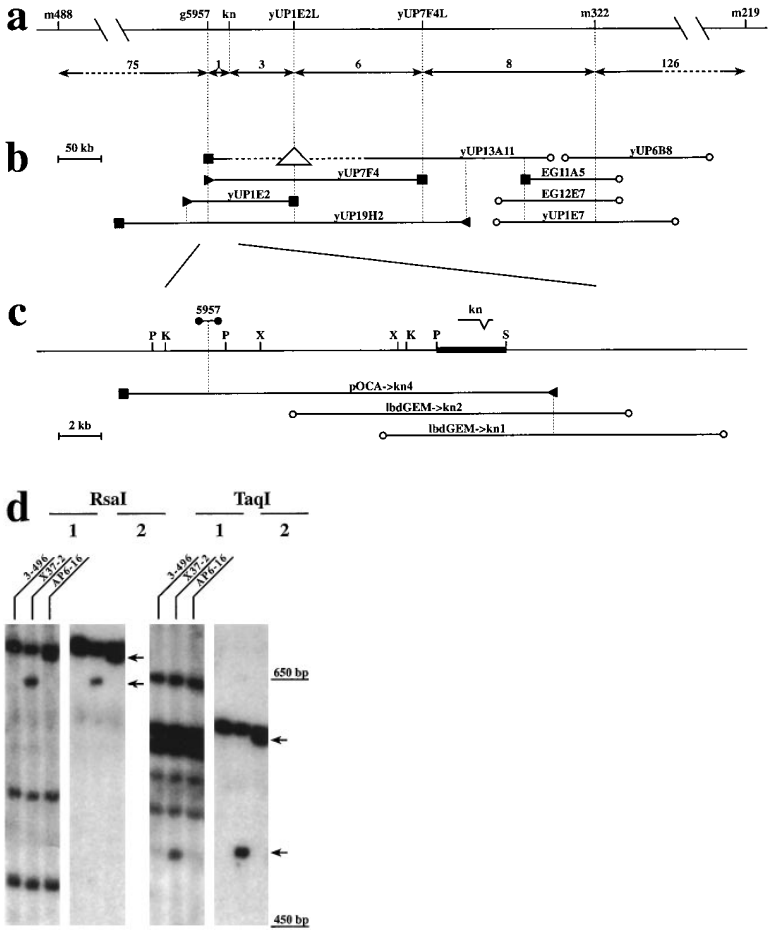

Figure 4. Positional Cloning of the *KN* Gene

(a) Genetic map of the *KN* region. Distances between molecular markers represent absolute numbers of recombinants.

(b) YAC contig. Dotted lines connect YAC clones with molecular probes that anchor and align them. Closed squares, right YAC ends; closed triangles, left ends; open circles, ends not aligned. The clone *yUP13A11* is likely to have an internal deletion (open triangle), since it does not include the right end of *yUP1E2*.

(c) Chromosome walk from CAPS *5957* to *KN*. The top line shows the approximate position of PstI (P), KpnI (K), XbaI (X), and SalI (S) restriction sites. The right end (closed square) of the cosmid clone pOCA→*kn4* does not hybridize to the YAC clones *yUP13A11* and *yUP1E2*, while its left end (closed triangle) does; both ends are included within the *g5957* cosmid.

(d) RFLPs associated with X-ray-induced *kn* alleles. TaqI and RsaI digests probed with λGEM→*kn1* (1) and the cDNA clone *w26* (2) are shown. Arrows indicate polymorphic bands detected in *X37-2* and *AP6–16*. No RFLP is detected in *3-496* heterozygous DNA.

clones isolated (pOCA→*kn4*) was mapped and did not give any recombinants with *KN*. A clone containing this left-end fragment (λGEM→*kn1*) was used to hybridize high resolution Southern blots of DNA from *kn*/+ plants. Allele-specific polymorphisms were detected in the DNAs from the two X-ray-induced alleles with various frequently cutting restriction enzymes (ten of 20 enzymes for each of the alleles; examples are shown in Figure 4d). All polymorphic bands were also detected using a central 3.4 kb SalI–PstI fragment of the same clone (highlighted in Figure 4c), whereas fragments on either side did not detect any polymorphism.

The central 3.4 kb fragment was used to isolate cDNA clones from flower- and silique-specific libraries. Positive clones were found at a frequency of about 1 in 1000. We analyzed in detail 11 clones falling into a single class. The two longest clones, about 1.2 kb in size, detected all allele-specific polymorphic bands on high resolution genomic blots of *kn*/+ heterozygous DNA (examples are shown in Figure 4d), suggesting that these cDNAs might represent *KN* mRNAs.

Sequence analysis of cDNAs and genomic DNAs from wild-type and mutant alleles confirmed that the *KN* gene had been cloned (Figure 5). The 5′ borders of the six longest cDNA clones lie within a region of about 80 bp; 5 nt upstream of the longest one there is a consensus transcriptional start site and a consensus TATA box, as described by Joshi (1987). All six clones have one or more stop codons in all possible frames preceding an ATG start codon that initiates an uninterrupted open reading frame encoding 310 amino acid residues. With a single exception (see Figure 5), the cDNAs isolated have virtually identical 3′ borders. Comparison with the genomic sequence reveals the presence of a single short intron within the 5′ untranslated region. The open reading frame represented by the cDNA clones is disrupted in all mutant alleles of *KN*. The EMS-induced allele *3-496* has a CG to AT transition that truncates the predicted KN protein at amino acid 71, the X-ray-induced allele *AP6-16* has a 4 bp deletion changing the reading frame from amino acid 198, and the X-ray-induced allele *X37-2* deletes the C-terminal one fourth of the coding sequence, as well as about 700 bp of downstream sequence. All these changes likely eliminate the activity of mutant KN proteins.

Similarity of the KN Gene Product to Syntaxins

The *KN* gene encodes a predicted 34 kDa protein with similarity to syntaxins, a family of proteins involved in vesicular trafficking (Figure 6). Syntaxins are thought to be target membrane receptors that specifically interact with corresponding vesicle receptors and soluble factors to promote eventually the fusion of target and vesicle membranes (for reviews see Bennett and Scheller, 1993; Südhof, 1995). Different types of syntaxins have

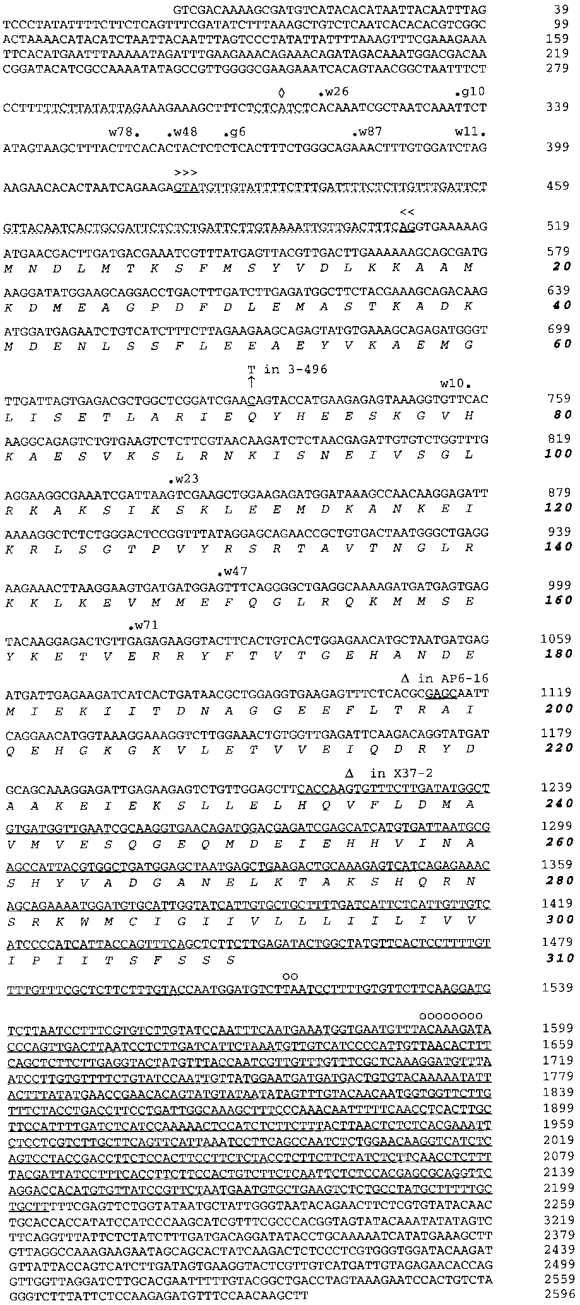

Figure 5. Sequence of the *KN* Gene

A consensus TATA box and a consensus transcriptional start around position 300 are underscored with a dotted line, and the putative transcriptional start site is marked with an open diamond. An intron between position 420 and 511 is underlined dotted; the conserved splice junctions are underlined and marked by arrows. AC to T transition in the allele *3-497* (position 730) and the nucleotides deleted in the alleles *AP6-16* (positions 1112–1115) and *X37-2* (positions 1216–2204) are underlined. The 5′ breakpoints of 11 cDNA clones examined are marked with dots, and their poly(A) ends are marked with open circles. With the exception of *w71*, the poly(A) sequences of all cDNA clones start within an 8 nt stretch around position 1595.

been implicated in a variety of trafficking pathways, such as docking and fusion of transmitter vesicles at the presynaptic membrane of neurons (syntaxin-1; Bennett et al., 1992; Inoue et al., 1992; Schulze et al., 1995), vesicular trafficking from the ER to the *cis*-Golgi compartment (SED5/syntaxin-5; Hardwick and Pelham, 1992; Dascher et al., 1994; Banfield et al., 1994), secretion to the plasma membrane (SSO1 and SSO2; Aalto et al., 1993; Jäntti et al., 1994), and secretion to the vacuole (PEP12; Preston et al., 1991; Bassham et al., 1995).

The predicted KN protein is similar to syntaxins in size and overall structure: it is predicted to form predominantly helical secondary structures and contains a C-terminal stretch of 24 hydrophobic amino acid residues that can potentially serve as a membrane anchor (Figure 6a). Sequence similarity among the syntaxins is most pronounced in the C-terminal region adjacent to the putative membrane anchor domain, for which 68 amino acid residues can be aligned without gaps, with six residues being identical in all members of the family (Figure 6b; Pelham, 1993). Within this stretch, KN shares 27%–39% identical amino acid residues with various syntaxins, including the only plant syntaxin reported, Arabidopsis PEP12, which is 27% identical to KN. All syntaxins have positively charged amino acid residues at the junction to the hydrophobic anchor, although their number and spacing varies among subgroups of syntaxins (Figure 6c). This feature has been implicated in membrane targeting of the proteins (Banfield et al., 1994). In comparison with the C-terminal region, the N-terminal regions of different syntaxins are more diverged.

It has been proposed that syntaxins interact with other proteins via coiled-coil structures (Pelham, 1993; Spring et al., 1993). Recombinant syntaxin-1 fragments bind factors of the membrane-docking and fusion complex in vitro, thereby defining interaction domains (Calakos et al., 1994; Kee et al., 1995). Most of the domains described map to the conserved C-terminal region that includes several heptad repeats of conserved hydrophobic amino acid residues characteristic for coiled-coil motifs (Figure 6b). However, according to the method of Lupas et al. (1991) for predicting coiled coils, the C-terminal region of KN has a low probability of forming coiled-coil structures (Figure 6a), as has also been noted previously for other syntaxins (Spring et al., 1993). By contrast, stretches within the N-terminal region of the KN protein have a high probability of forming coiled coils (Figure 6a). Heptad repeats related to one of these putative domains, positions 94 to 121, are present in other syntaxins (Spring et al., 1993) and have been referred to as helix 2 in syntaxin-1 (Kee et al., 1995).

We performed a phylogenetic analysis to determine how KN is related to the various syntaxins (Figure 6c). Groups of syntaxins that serve similar functions in distantly related organisms are found on the same branch of the phylogenetic tree, such as syntaxin-1 from mammals, insects, and mollusks, SED5/syntaxin-5 from mammals, insects, and budding yeast, or PEP12 from plants and budding yeast. It is difficult, however, to relate these evolutionarily ancient branches to each

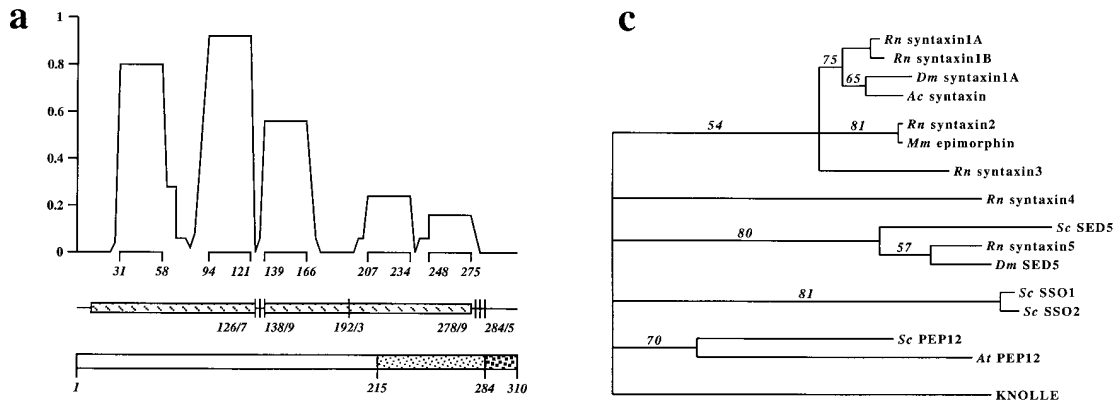

b

		a d a d a d a d a d a d a d	% identical to KNOLLE
Rn syntaxin1A	195	IETRHSEIIKLENSIRELHDMFMDMAMLVESQGEMIDRIEYNVEHAVDYVERAVSDTKKAVKYQSKARRKK*IMIIICCVILGIIIASTIGGIPG*	39
Rn syntaxin1B	194	IETRHNEIIKLETSIRELHDMFVDMAMLVESQGEMIDRIEYNVEHSVDYVERAVSDTKKAVKYQSKARRKK*IMIIICCVVLGVVLASSIGGTLGL*	37
Dm syntaxin1A	198	IEARHQDIMKLETSIKELHDMFMDMAMLVESQGEMIDRIEYHVEHAMDYVQTATQDTKKALKYQSKARRKK*IMILICLTVLGILAASYVSSYFM*	39
Ac syntaxin	196	IEARHNDIMKLETSIRDLHDMFMDMAMLVESQGEMIDRIEYNVEQAVDYIETAKNDTKKAVKYQSKARRKK*IMILVCLAILIIILVGVIGGTLG*	34
Rn syntaxin2	196	IESRHKDIMKLETSIRELHEMFMDMAMFVETQGEMVNNIERNVVNSVDYVEHAKEETKKAIKYQSKARRKK*WIIAAVVVAVIAVLALIIGLTVGK*	34
Mm epimorphin	195	IESRHKDIMKLETSIRELHEMFMDMAMFVETQGEMVNNIERNVVNSVDYVEHAKEETKKAIKYQSKARRKK*WIIAAVAVAVIAVLALIIGLSVGK*	35
Rn syntaxin3	194	IEGRHKDIVRLESSIKELHDMFMDIAMLVENQGEMLDNIELNVMHTVDHVEKARDETKRAMKYQGQARKK*LIIIIVIVVVLLGILALIIGLSVGLK*	37
Rn syntaxin4	203	ISARHSEIQQLERTIRELHEIFTFLATEVEMQGEMINRIEKNILSSADYVERGQEHVKIALENQKKARKKK*VMIAICVSVTVLILAVIIGITITTVG*	32
Sc SED5	252	LQERNRAVETIESTIQEVGNLFQQLASMVQEQGEVIQRIDANVDDIDLNISGAQRELLKYFDRIKSNRWLAAK*VFFIIFVFFVIWVLVN*	27
Rn syntaxin5	211	IQSRADTMQNIESTIVELGSIFQQLAHMVKEQEETIQRIDENVLGAQLDVEAAHSEILKYFQSVTSNRWLMVK*IFLILIVFFIIFVVFLA*	31
Dm SED5	221	VQQRAETMQNIESTIVELGGIFQQLAHMVKEQEEIVERIDTNVADAELNIEAAHGEILKYFQSVSKNRWLMIK*IFGVLIFFFLFFVVFMS*	27
Sc SSO1	193	VQARHQELLKLEKSMAELTQLFNDMEELVIEQQENVDVIDKNVEDAQLDVEQGVGHTDKAVKSARKARKNKIRC*WLIVFAIIVVVVVVVVVPAVVKTR*	33
Sc SSO2	197	VQARHQELLKLEKTMAELTQLFNDMKELVIEQQENVDVIDKNVEDAQQDVEQGVGHTNKAVKSARKARKNKIRC*LIICFIIFAIVVVVVVVVPSVVETRK*	32
Sc PEP12	198	IEQRDQEISNIERGITELNEVFKDLGSVVQQQGVLVDNIEANIYTTSDNTQLASDELRKAMRYQKRTSRWRVYLLIVLLVMLLFIFLIMKL	29
At PEP12	199	IEEREQGIREIEDQIRDVNGMFKDLALMVNHQGNIVDDISSNLDNSHAATTQATVQLRKAAKTQRSNSSLTC*LLILIFGIVLLIVIIVVLV*	27
KNOLLE	215	IQDRYDAAKEIEKSLLELHQVFLDMAVMVESQGEQMDEIEHHVINASHYVADGANELKTAKSHQRNSRKWMC*IGIIVLLLIILIVVIPIITSFSSS*	100
invariant		* R E F V Q I *	

Figure 6. Similarity of the KN Gene Product to Syntaxins

(a) Structural features of the predicted KN protein. At the top, probability of coiled coil formation as calculated after Lupas et al. (1991). Middle, Robson/Garnier predictions on the secondary structure. Bars represent putative helical regions, and vertical lines represent putative turns. Bottom, putative membrane anchor (closed squares) and the conserved region (dots) listed in (b).

(b) Conserved C-terminal region of syntaxins (modified after Pelham, 1993; Spring et al. 1993; Banfield et al., 1994). *Ac*, *At*, *Dm*, *Mm*, *Rn*, and *Sc* designate sequences isolated from Aplysia, Arabidopsis, Drosophila, mouse, rat, and budding yeast, respectively. The position of the first residue is listed on the left. A putative membrane anchor domain (italics) is preceded by a cluster of positively charged residues (bold). The top line shows conserved regularly spaced hydrophobic positions (a and d) of nine heptad repeat units. The bottom line shows six invariant residues contained in a conserved 68 residue region (indicated by asterisks) that can be aligned without gaps. Percent identities of this region are shown on the right. The GenBank accession number for Aplysia syntaxin is U03123; the sequence for mouse epimorphin is taken from Hirai et al. (1992); the SwissProt accession number for budding yeast PEP12 is P32854; for other references, see text.

(c) Phylogenetic tree of the syntaxin family. The tree was generated by neighbor joining on the basis of the conserved C-terminal region that can be aligned without gaps (see asterisks in [b]). Multiple substitutions were corrected for according to the method of Kimura (1983). Numbers refer to confidence values for the respective branches as determined by 2000 bootstrap replicates. Only branches with a confidence value of greater than 50 are shown. Similar, although not identical, results were obtained when the calculations were performed on the basis of the complete amino acid sequences or when trees were generated by maximum parsimony (data not shown). Syntaxin-3 is sometimes separated from syntaxin-1/2, whereas syntaxin-4 is sometimes placed close to the syntaxin-1/2/3 group.

other. KN is not closely related to any one of the other syntaxins. This suggests that KN is a novel member of the syntaxin family.

Transcription of the *KN* Gene in Embryos

To relate the phenotypic effects of *kn* mutations to the expression of the *KN* gene in wild type, we analyzed the accumulation of *KN* RNA during development (Figure 7). On Northern blots, a probe covering the *KN* coding sequence detects a single band of about 1.3 kb. *KN* RNA is most abundant in flowers and developing siliques, while comparatively little is detectable in seedlings, roots, and leaves (Figures 7a and 7b).

The expression pattern of *KN* RNA in developing embryos was determined by in situ hybridization to tissue sections (Figures 7d–7i). *KN* transcripts are detected throughout embryogenesis until expression declines in the mature embryo (Figure 7i). Expression was observed in all tissues examined, but only single cells or small groups of adjacent cells accumulate *KN* RNA. This patchy pattern is invariantly found for all stages analyzed, from the 8-cell stage to the bent-cotyledon stage (Figures 7d–7h). Occasionally, two or three adjacent cells in a file of vascular precursors showed similar levels of *KN* expression (data not shown). The intensity of the signals varies among positive cells in a given section (for example see Figure 7e), suggesting that the *KN* RNA turns over asynchronously in different cells. Our observations are consistent with the notion that *KN* transcripts are produced only during a specific phase of the cell cycle.

Discussion

The *KN* Gene Is Involved in Cytokinesis

Incomplete and misoriented cell divisions become apparent very early in the development of *kn* embryos. However, the cells increase in size, expanding the surface area of both plasma membranes and cell walls. Tip growth is also normal, as judged from the development

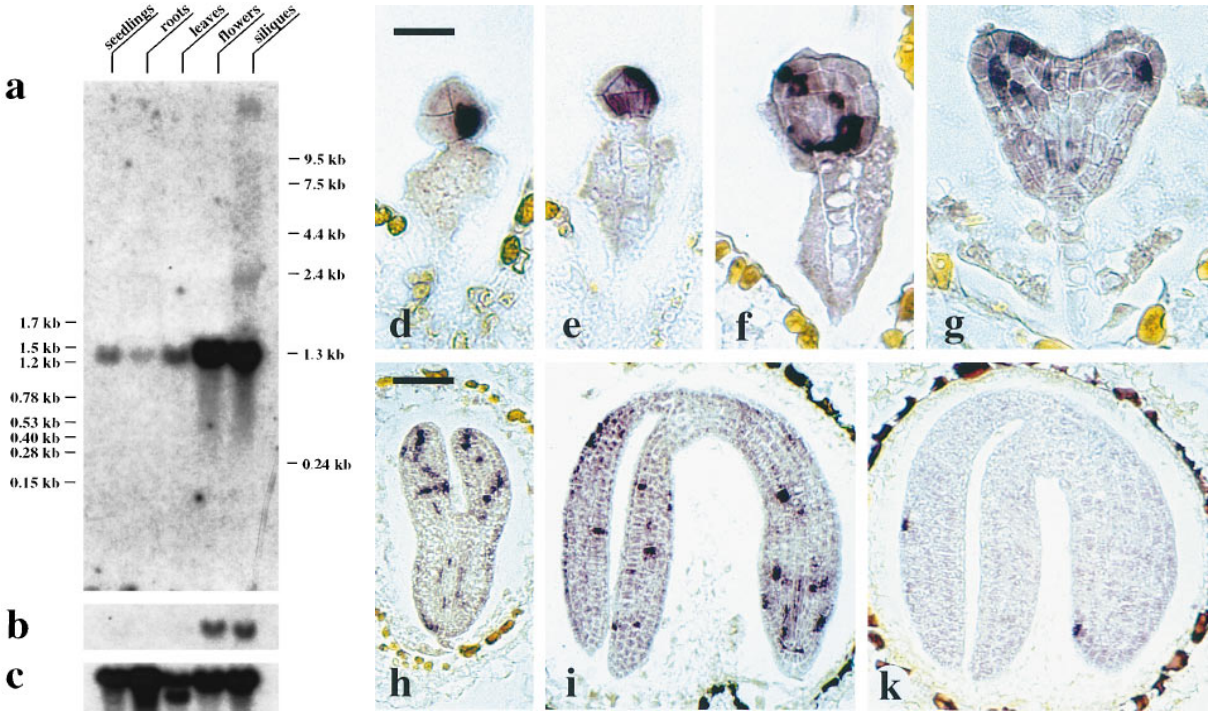

Figure 7. Analysis of *KN* Gene Expression

(a and b) Northern blot analysis. About 25 μg of total RNA prepared from the tissue indicated was loaded in each lane; length standards are shown on both sides. A PCR fragment covering the complete coding sequence was used for hybridization. Exposures were 14 days for (a) and 2 days for (b).

(c) Loading control. Shown is the same filter hybridized with a polyubiquitin coding sequence that detects multiple bands of differing intensities (Burke et al., 1988; Trezzini et al., 1993). Only the two most prominent bands are visible. Exposure was 4 hr.

(d–k) In situ hybridization to wild-type embryos. Sections were hybridized with a riboprobe from the 3′ end of the *KN* coding sequence (see Experimental Procedures). (d), 8-cell stage; (e), dermatogen; (f), globular; (g), heart; (h), torpedo; (i), bent cotyledon; and (k), mature embryo. Scale bar is 50 μm in (d)–(g) and 100 μm in (h)–(k).

of root hairs and pollen tubes. Thus, the general cellular machinery for synthesis and deposition of cell surface material appears unaffected. A specific function of the *KN* gene in cell division is suggested by the accumulation of *KN* RNA in patches of single cells or small groups of cells. A similar expression pattern has been observed for a number of cell-cycle genes, such as histone H2 in side shoots and side roots of tomato (Koning et al., 1991) and histone H4 and a mitotic cyclin in the shoot apex of Antirrhinum (Fobert et al., 1994). Since embryonic cell divisions are not synchronous, *KN* expression is likely confined to a brief period during the cell cycle, suggesting that the KN protein has to be available in sufficient amounts at a specific time.

The cellular phenotype of *kn* embryos is pleiotropic. Cells are enlarged and often contain two or more polyploid nuclei that are separated by cytoplasm but by neither a cross wall nor a plasma membrane. Polyploidy and the occurrence of variably multinucleate cells are features of cytokinesis-defective mutants in a number of organisms (Karess et al., 1991; Harris et al., 1994; Neufeld and Rubin, 1994; Simanis, 1995). In the case of Drosophila *pebble* mutants, the sequence of events resulting in a nuclear phenotype similar to *kn* has been described in some detail (Hime and Saint, 1992; Lehner, 1992): *pebble* embryos fail to form contractile rings required for cytokinesis past the blastoderm stage. The cells contain two nuclei initially, but then additional rounds of DNA replication occur, and the cells enlarge. However, a variable number of mitotic spindles is formed in these divisions, resulting in either multinucleate cells or nuclear restitution and polyploidy. By analogy, the pleiotropic cellular phenotype of *kn* embryos most likely reflects a primary defect in cytokinesis.

In *kn* embryos, the number of cells continues to increase during development, although at a much reduced rate, indicating that the cell division defect can be bypassed. It is possible that some other component involved in cytokinesis functionally overlaps with the KN protein. Alternatively, cytokinesis may be achieved by different mechanisms, with KN being required for only one of them. The latter possibility is suggested by the observation that cross wall fragments are attached to the parental wall, as will be discussed below.

Cytokinesis and Radial Pattern Formation

In the Arabidopsis embryo, the radial pattern originates in a series of oriented cell divisions that produce concentrically arranged layers of tissue primordia (Mansfield and Briarty, 1991; Jürgens and Mayer, 1994). No such oriented divisions are observed in *kn* embryos, and the concentric arrangement of tissue layers is not apparent in *kn* seedlings. However, *kn* seedlings generally display cellular differentiation markers for all major tissue types

in a spatial order similar to that in wild-type seedlings. An evident exception are cells at the surface that variably take on features of subepidermal cells, such as the accumulation of anthocyanin.

Three aspects of development that are altered in *kn* embryos could account for the radial pattern defect: abnormal planes of cell divisions, reduced cell numbers, and incomplete separation of daughter cells. A highly irregular pattern of cell divisions has been described for Arabidopsis *fass* embryos (Torres Ruiz and Jürgens, 1994). However, *fass* seedlings differentiate a complete and fully functional array of tissues, suggesting that oriented cell divisions are not instrumental for radial patterning, but rather reflect the process. A shortage of cells causes a radial pattern defect in Arabidopsis *wooden leg* seedlings, which lack the phloem cells of the centrally located vascular tissue (Scheres et al., 1995). This defect can be suppressed by mutations in the *FASS* gene that increase the number of cells across the tissue layers. Thus, neither abnormal planes of cell divisions nor reduced cell numbers can alone explain the radial pattern defect of *kn* seedlings.

Incomplete cytokinesis as seen in *kn* embryos generates groups of interconnected cells that may freely exchange information. Although it is not known what role uncoupling of cells or cell populations plays in plant embryogenesis, one could imagine that the identity of cells within a given tissue might be maintained by uncoupling them from neighboring cells of a different tissue. This idea is based on the finding that fluorescent dye taken up by hypocotyl cells of Arabidopsis seedlings readily spreads within the epidermis, but not into the underlying ground tissue (Duckett et al., 1994). By analogy, the accumulation of anthocyanin in a minority of surface cells observed in *kn fus* double mutant seedlings might reflect incomplete separation of adjacent tissues due to defective cytokinesis.

The KN Protein: A Cytokinesis-Specific Syntaxin?

In flowering plants, cross walls typically grow from a cell plate in the center of the plane of division toward the periphery to fuse with the parental wall. However, cross walls formed after meiosis have been reported to grow in from the parental walls in the majority of dicot plants, including Arabidopsis (Maheshwari, 1950; Owen and Makaroff, 1995). In the alga Spirogyra, two separate mechanisms, actin-based cleavage initiated at the parental wall and microtubule-dependent formation of a cell plate in the center, combine to achieve cytokinesis. If the microtubules are destabilized by drug treatment, cytokinesis is initiated at the periphery, but is not completed, leaving a gap in the center of the cross wall (McIntosh et al., 1995). This defect is reminiscent of the incomplete cell divisions in *kn* embryos, in which fragments of cross walls are found attached to the parental cell wall. We speculate that these fragments might represent cross walls that were generated independently of a cell plate.

The cell plate is formed by the accumulation and fusion of Golgi-derived vesicles (reviewed by Wick, 1991; Hepler and Newcomb, 1967). This process is affected by caffeine in a variety of species (reviewed by Gunning, 1982). If root meristems of bean seedlings are incubated with caffeine, dividing cells fail to generate a cell plate and instead produce extensions of the parental wall (Röper and Röper, 1977). After prolonged treatment, the cells are separated by incomplete cross walls and are enlarged, containing multiple as well as polyploid nuclei. The alterations of cytokinesis caused by caffeine have been resolved in a temporal sequence for dividing stamen hair cells from the flowering plant Tradescantia (Hepler and Bonsignore, 1990): Golgi-derived vesicles align normally at the position of the newly forming cell plate, and some fusion into larger aggregates occurs; however, maturation of a cell plate fails, and the vesicles are eventually resorbed, leaving no trace of a cell plate. A very recent study described a pea mutant named *cytokinesis-defective* (*cyd*) that has a cellular phenotype similar to *kn* (Liu et al., 1995). The authors also showed that the cytokinesis defect of the *cyd* mutant can be mimicked by caffeine treatment of wild-type pea seedlings and discuss a possible function of the *Cyd* gene in the vesicular transport system. These observations suggest a link between the molecular function of the *KN* gene and the cytokinesis defects of *kn* embryos. Based on its similarity to syntaxins, the predicted KN protein is likely involved in some aspect of vesicular trafficking or membrane fusion. Considering the similarity of the cytokinesis defects caused by caffeine treatment and by mutation in *KN*, we propose that the KN gene product might act as a cell plate–specific syntaxin, facilitating the transport of vesicles to, or their fusion at, the plane of cell division. This idea can be put to test when KN-specific antibodies become available.

Recently, a role in protein secretion has been discussed for another gene, *GNOM*/*EMB30*, identified in a screen for embryonic pattern mutants of Arabidopsis (Mayer et al., 1991), because its product shares a stretch of nearly 200 amino acids (the "Sec7 domain") with the yeast secretory protein Sec7p (Shevell et al., 1994). Although the two genes, *GNOM* and *KN*, seem to act in related cellular processes, several observations suggest that their biological roles are distinct. Unlike *KN*, *GNOM* is involved in apical–basal pattern formation (Mayer et al., 1993), and the two genes act independently, as shown by double mutant analysis (U. M., unpublished data). Furthermore, *gnom*, but not *kn*, cells divide vigorously in tissue culture, giving rise to callus (Mayer et al., 1993). It would thus appear premature to speculate about a general significance of protein secretion in early plant development.

Experimental Procedures

Genetic Techniques and Phenotypic Analysis

The *kn* alleles *3-496* and *X37-2* have been described previously (Mayer at al., 1991); the allele *AP6-16* was isolated from the F2 of *an dis1; ap3-1* crossed with X-rayed *Landsberg* (*Ler*) pollen (20,000 rads; U. M. and W. L., unpublished data). *an dis1* and *ap3-1* have been described by Koornneef and Hanhart (1983) and Bowman et al. (1989). *kn fus* double mutant embryos did not germinate and were dissected from the ovule prior to desiccation; the progeny of three crosses, *fus1 3-16* to *knX37-2*, *kn3-496* to *fus1 3-16*, and *fus2 R16-11* to *knX37-2*, showed similar phenotypes (also including early embryonic lethality). The *fus* mutants have been described by Miséra et al. (1994). For dark-field microscopy, seedlings were cleared with

chloral hydrate (Mayer et al., 1991). For nuclear staining with YO-PRO-1 iodide (1:1000; Molecular Probes, Eugene, OR), embryos were prepared after Goodbody and Lloyd (1994). Plastic sections of embryos were prepared as described previously (Mayer et al., 1993). Specimens for electron microscopy were fixed as for light microscopy, postfixed with 1% OsO_4 for 2 hr at room temperature, and contrasted with 1% uranyl acetate for 1 hr in the refrigerator; ultrathin 70–80 nm sections of embryos were analyzed with a Philips CM10 transmission electron microscope. All images shown were processed with the Photoshop software (Adobe, Mountain View, CA).

Molecular Mapping of *KN*

For molecular mapping, 734 F2 plants from a cross of *kn X37-2* to *Niederzenz* (*Nd-0*) and 614 from a cross of *kn 3-496* to *Nd-0* were examined; the overall recombination frequency in the first population was about twice that in the second population. Genomic DNA for RFLP mapping was prepared as described by Leutwiler et al. (1984). To prepare genomic DNA for PCR, single rosette leaves were mashed and incubated with 0.2 ml of CTAB buffer at 65°C for 1 hr; the mixture was extracted with chloroform, and the nucleic acids contained in the aqueous phase were precipitated (Rogers and Bendich, 1988; F. Assaad and G. J., unpublished data). Reaction conditions and procedures were as follows: CAPS *488*, primer pair 5′-CAA CTA TTT GTT CAC GGG C-3′ and 5′-CGT ATC ACT AAC AAC GGT CC-3′; 40 cycles; 50°C annealing temperature; standard Taq buffer. The PCR amplifies a 0.7 kb fragment that contains a single HindIII site present in *Nd-0* and absent in *Ler*. CAPS *5957*, primer pair 5′-ACT TCC GAA CCA TAT GG-3′ and 5′-CAA ATT CTC TGA CCT GGC C-3′; 40 cycles; 55°C annealing temperature; 1.5 mM $MgCl_2$, 75 mM KCl, 10 mM Tris (pH 8.8) reaction buffer. The PCR amplifies a 1.3 kb fragment that contains a single HincII site present in *Ler* and absent in *Nd-0*. CAPS *322*, primer pair 5′-AGA GTG GCA GTT GGC ATA-3′ and 5′-GGA CAG TGA TAC AAC A-3′; 40 cycles; 55°C annealing temperature; standard Taq buffer. The PCR amplifies a 0.7 kb fragment from *Ler* DNA and a 0.5 kb fragment from *Nd-0* DNA. CAPS *219*, primer pair 5′-TCC TTA ATC CCG TTC CTC-3′ and 5′-CTG ATC GCT AAT GGG TG-3′; 35 cycles; annealing temperature 55°C; standard Taq buffer. The PCR amplifies a 1.3 kb fragment from *Ler* DNA and a 1.1 kb fragment from *Nd-0* DNA.

Molecular Cloning

Routines were performed as described by Sambrook et al. (1989). YAC end probes were generated by modified vectorette PCR as described by Matallana et al. (1992). For *EG* clones, the following nested primers were used (T. Debener and J. Dangl, personal communication): 5′-GCA ATT AAC CCT CAC TAA AG-3′ (left end) and 5′-CGC AAT TAA CCC TCA CTA TAG-3′ (right end). A λGEM library prepared by G. Mulligan and R. Davis (Stanford University), a λDASHII library prepared by D. Coates (University of Leeds; both libraries have been deposited in the Arabidopsis stock center), and a pOCA cosmid library, described by Olszewski et al. (1988), were used to isolate *KN* genomic clones. For the detection of RFLPs associated with mutant *kn* alleles, heterozygous DNA was digested with 20 different restriction enzymes that have 4 or 5 nt recognition sites, and blots were prepared as described by Gebhardt et al. (1989); as determined by hybridization with a known sequence, the blots allow for the detection of length polymorphisms as small as 5 bp in a 500 bp background (data not shown). *KN* cDNAs were isolated from libraries of young inflorescences (*w* clones; Weigel et al., 1992) and siliques (*g* clones; Giraudat et al., 1992). The primer pair 5′-CAC TAC TCT CTC ACT TTC TGG GC-3′ and 5′-ATT GGA TAC AAG ACA CGA AAG G-3′ was used to amplify the coding sequence of the *kn* alleles *3-496* and *AP6-16* (40 cycles; annealing temperature 58°C; reaction buffer, 1.5 mM $MgCl_2$, 25 mM KCl 10 mM Tris (pH 9.2); the PCR amplifies a 1.2 kb fragment). In the *X37-2* chromosome there is a deletion of about 1 kb that maps between the BglII site around position 793 and the HindIII site around position 2590 (data not shown). The primer pair 5′-GCA GAG TCT GTG AAG TCT CTT CG-3′ and 5′-CTG CAT GAG TTC CAC ACA GAA GG-3′ was used to amplify the breakpoints of this deletion (35 cycles; annealing temperature 65°C; standard Taq buffer; a 0.5 kb fragment is amplified from *X37-2* and a 1.5 kb fragment from *Ler*). Plasmids containing inserts from different PCR reactions were generated using a T-cloning kit (MBI/Fermentas, Vilnius, Lithuania) and analyzed by sequencing. Subclones of λGEM→*kn1 and* λ*GEM→kn2* were used to determine the *KN* genomic sequence. With the exception of a small intron in the 5′ untranslated leader absent in both clones, no deviations from the genomic sequence were found in the two longest cDNA clones, *w26* and *g10*. Of the remaining cDNA clones, only the borders were sequenced; two clones, *w26* and *w48*, contain 38 and 19 bp at their 5′ border, respectively, that do not have a counterpart in the *KN* genomic sequence; these sequences are characterized by repeats of CT or AG and are likely due to a cloning artifact.

Computer Analysis

Predictions of the secondary structure were determined with the MacVector software (Kodak Scientific Imaging Systems, New Haven, CT). Database searches were done using the BLAST e-mail server at the National Center for Biotechnology Information (blast@ncbi.nlm.nih.gov). Phylogenetic trees were generated with ClustalV and PAUP software (Higgins et al., 1992; Swofford, 1993).

Analysis of *KN* Expression

For Northern blots, RNA was prepared according to Timberlake (1986). In situ hybridizations were performed as described by Cox and Goldberg (1988). A 200 bp HincII–BglI fragment (position 558 to 793) and a 300 bp subfragment of the clone *w71* truncated with PflMI (position 1308) were used for in vitro transcription with DIG-rUTP (Boehringer–Mannheim, Mannheim, FRG; sense transcripts, T3 promoter; antisense transcripts, T7 promoter). Both probes gave similar results. DIG epitopes were detected using a Boehringer kit (anti-DIG FAB fragment coupled to alkaline phosphatase with NBT and X phosphate as substrates; staining reaction overnight).

Acknowledgments

Marker strains, libraries, clones, and protocols were kindly provided by M. Koornneef; J. Dangl, T. Debener, U. Hartmann, and B. Weisshaar; J. Giraudat; N. Olszewski; D. Weigel; F. Schauwecker, M. Urban, and R. Schwabe. F. Assaad and M. Busch kindly shared the protocols for plant DNA minipreps and the CAPS *219* and *322*. E. Matallana, P. Dunn, and J. Ecker made available unpublished information about YAC clones. C. Gebhard and B. Walkemeier helped preparing the high resolution Southern blots. M. Bähler and H.-E. Stöffler calculated the coiled coil probability. D. Bassham and N. Raikhel communicated the aPEP12 sequence prior to publication. C. Schlötterer and M. Friedrichs helped with the phylogenetic analysis. I. Waizenegger prepared the nuclear stains. I. Zimmermann and H. Schwartz helped with the electron microscopic analysis. We are grateful to K. Boutillier, C. Vroemen, M. Hartog, S. C. DeVries, and their colleagues for hospitality, discussion, and help with the in situ hybridization. We thank our colleagues in Tübingen and Munich for critical reading of the manuscript. Initial support was provided by Deutsche Forschungsgemeinschaft grant Ju 179/2-2. W. L. was supported by short-term fellowships from the Boehringer–Ingelheim Stiftung (Stuttgart) and the Agricultural University Wageningen (The Netherlands). This work was funded in part by the European Community's BIOTECH Programme, as part of the Project of Technological Priority 1993–1996.

Received August 30, 1995; revised November 3, 1995.

References

Aalto, M.K., Ronne, H., and Keränen, S. (1993). Yeast syntaxins Sso1p and Sso2p belong to a family of related membrane proteins that function in vesicular transport. EMBO J. *12*, 4095–4104.

Asada, T., and Shibaoka, H. (1994). Isolation of polypeptides with microtubule-translocating activity from phragmoplasts of tobacco BY-2 cells. J. Cell Sci. *107*, 2249–2257.

Banfield, D.K., Lewis, M.J., Rabouille, C., Warren, G., and Pelham, H.R.B. (1994). Localization of Sed5, a putative vesicle targeting molecule, to the cis-Golgi network involves both its transmembrane and cytoplasmatic domains. J. Cell Biol. *127*, 357–371.

Bassham, D.C., Gal, S., Da Silva Conceiçao, A., and Raikhel, N.V. (1995). An *Arabidopsis* syntaxin homologue isolated by functional complementation of a yeast *pep12* mutant. Proc. Natl. Acad. Sci. USA *92*, 7262–7266.

Bennett, M.K., Calakos, N., and Scheller, R.H. (1992). Syntaxin: a synaptic protein implicated in docking of synaptic vesicles at presynaptic active zones. Science *257*, 255–259.

Bennett, M.K., García-Arrarás, J.E., Elferink, L.A., Peterson, K., Fleming, A.M., Hazuka, C.D., and Scheller, R.H. (1993). The syntaxin family of vesicular transport receptors. Cell *74*, 863–873.

Bowman, J.L., Smyth, D.R., and Meyerowitz, E.M. (1989). Genes directing flower development in *Arabidopsis*. Plant Cell *1*, 37–52.

Burke, T.J., Callis, J., and Vierstra, R.D. (1988). Characterization of a polyubiquitin gene from *Arabidopsis thaliana*. Mol. Gen. Genet. *213*, 435–443.

Calakos, N., Bennett, M.K., Peterson, K.E., and Scheller, R.H. (1994). Protein-protein interactions contributing to the specificity of intracellular vesicular trafficking. Science *263*, 1146–1149.

Cox, K.H., and Goldberg, R.B. (1988). Analysis of plant gene expression. In Plant Molecular Biology: A Practical Approach, C.H. Shaw, ed. (Oxford: IRL Press), pp. 1–34.

Dascher, C., Matteson, J., and Walch, W.E. (1994). Syntaxin5 regulates endoplasmatic reticulum to Golgi transport. J. Biol. Chem. *269*, 29363–29366.

Duckett, C.M., Oparka, K.J., Prior, D.A.M., Dolan, L., and Roberts, K. (1994). Dye-coupling in the root epidermis of *Arabidopsis* is progressively reduced during development. Development *120*, 3247–3255.

Fishkind, D.J., and Wang, Y.-L. (1995). New horizons for cytokinesis. Curr. Biol. *7*, 23–31.

Fobert, P.F., Coen, E.S., Murphy, G.J.P., and Doonan, J.H. (1994). Pattern of cell division revealed by transcriptional regulation of genes during the cell cycle in plants. EMBO J. *13*, 616–624.

Gebhardt, C., Ritter, E., Debener, T., Schachtschabel, U., Walkemeier, B., Uhrig, H., and Salamini, F. (1989). RFLP analysis and linkage mapping in *Solanum tuberosum*. Theor. Appl. Genet. *78*, 65–75.

Giraudat, J., Hauge, B.M., Valon, C., Smalle, J., Parcy, F., and Goodman, H.M. (1992). Isolation of the *Arabidopsis* ABI3 gene by positional cloning. Plant Cell *4*, 1251–1261.

Goodbody, K.C., and Lloyd, C.W. (1994). Immunofluorescence techniques for analysis of the cytoskeleton. In Plant Cell Biology: A Practical Approach, N. Harris and K.J. Oparka, eds. (Oxford: IRL Press), pp. 221–243.

Gunning, B.E.S. (1982). The cytokinetic apparatus: its development and spacial regulation. In The Cytoskeleton in Plant Growth and Development, C.W. Lloyd, ed. (New York: Academic Press), pp. 230–288.

Hardwick, K.G., and Pelham, H.R.B. (1992). SED5 encodes a 39-kD integral membrane protein required for vesicular transport between the ER and the Golgi complex. J. Cell Biol. *119*, 513–521.

Harris, S.D., Morrell, J.L., and Hamer, J.E. (1994). Identification and characterization of *Aspergillus nidulans* mutants defective in cytokinesis. Genetics *136*, 517–532.

Hauge, B.M., Hanley, S.M., Cartinhour, S., Cherry, J.M., Goodman, H.M., Koornneef, M., Stam, P., Chang, C., Kempin, S., Medrano, L., and Meyerowitz, E.M. (1993). An integrated genetic/RFLP map of the *Arabidopsis thaliana* genome. Plant J. *3*, 745–754.

Hepler, P.K., and Bonsignore, C.L. (1990). Caffeine inhibition of cytokinesis: ultrastructure of cell plate formation/degradation. Protoplasma *157*, 182–192.

Hepler, P.K., and Newcomb, E.H. (1967). Fine structure of cell plate formation in the apical meristem of *Phaseolus* roots. J. Ultrastruct. Res. *19*, 498–513.

Higgins, D.G., Bleasby, A.J., and Fuchs, R. (1992). CLUSTAL V: improved software for multiple sequence alignment. Comp. Appl. Biosci. *8*, 189–191.

Hime, G., and Saint, R. (1992). Zygotic expression of the *pebble* locus is required for cytokinesis during the postblastoderm mitoses of *Drosophila*. Development *114*, 165–171.

Hirai, Y., Takebe, K., Takashina, M., Kobayashi, S., and Takeichi, M. (1992). Epimorphin: a mesenchymal protein essential for epithelial morphogenesis. Cell *69*, 471–481.

Hwang, I., Kohchi, T., Hauge, B.M., and Goodman, H.M., Schmidt, R., Cnops, C., Dean, C., Gibson, S., Iba, K., Arondel, V., Danhoff, L., and Somerville, C. (1991). Identification and map position of YAC clones comprising one third of the *Arabidopsis genome*. Plant J. *1*, 367–374.

Inoue, A., Obata, K., and Akagawa, K. (1992). Cloning and sequence analysis of the cDNA for a neuronal cell membrane antigen, HPC-1. J. Biol. Chem. *267*, 10613–10619.

Jäntti, J., Keränen, S., Toikkanen, J., Kuismanen, E., Ehnholm, C., Sönderlund, H., and Olkkonen, V.M. (1994). Membrane insertion and intracellular transport of yeast syntaxin Sso2p in mammalian cells. J. Cell Sci. *107*, 3623–3633.

Joshi, C.P. (1987). An inspection of the domain between putative TATA box and translational start site in 79 plant genes. Nucl. Acids Res. *15*, 6643–6651.

Jürgens, G., and Mayer, U. (1994). *Arabidopsis*. In Embryos: Colour Atlas of Development, J.B.L. Bard, ed. (London: Wolfe Publishers), pp. 7–21.

Karess, R.E., Chang, X.-J., Edwards, K.A., Kulkarni, S., Aguilera, I., and Kienhart, D.P. (1991). The regulatory light chain of nonmuscle myosin is encoded by *spaghetti-squash*, a gene required for cytokinesis in Drosophila. Cell *65*, 1177–1189.

Kee, Y., Lin, R.C., Hsu, S.-C., and Scheller, R. (1995). Distinct domains of syntaxin are required for synaptic vesicle fusion complex formation and dissociation. Neuron *14*, 991–998.

Kimura, M. (1983). The Neutral Theory of Molecular Evolution (Cambridge: Cambridge University Press).

Koning, A.J., Tanimoto, E.Y., Kiehne, K., Rost, T., and Comai, L. (1991). Cell-specific expression of plant histone H2A genes. Plant Cell *3*, 657–665.

Koornneef, M., and Hanhart, C.J. (1983). Linkage marker stocks of *Arabidopsis thaliana*. Arabid. Info. Serv. *20*, 89–92.

Lambert, A.-M. (1993). Microtubule-organizing centers in higher plants. Curr. Opin. Cell Biol. *5*, 116–122.

Lehner, C.F. (1992). The pebble gene is required for cytokinesis in *Drosophila*. J. Cell Sci. *103*, 1021–1030.

Leutwiler, L.S., Hough-Evans, B.R., and Meyerowitz, E.M. (1984). The DNA of *Arabidopsis thaliana*. Mol. Gen. Genet. *194*, 15–23.

Liu, C.-M., Johnson, S., and Wang, T.L. (1995). *cyd*, a mutant of Pea that alters embryo morphology, is defective in cytokinesis. Dev. Genet. *16*, 321–331.

Lupas, A., Van Dyke, M., and Stock, J. (1991). Predicting coiled coils from protein sequences. Science *252*, 1162–1164.

Maheshwari, P. (1950). An Introduction to the Embryology of Angiosperms (New York: McGraw–Hill).

Mansfield, S.G., and Briarty, L.G. (1991). Early embryogenesis in *Arabidopsis thaliana*. II. The developing embryo. Can. J. Bot. *69*, 461–476.

Matallana, E., Bell, C.J., Dunn, P.J., Lu, M., and Ecker, J.R. (1992). Genetical and physical linkage of the *Arabidopsis* genome: methods for anchoring yeast artificial chromosomes. In Methods in *Arabidopsis* Research, C. Koncz, N.-H. Chua, and J. Schell, eds. (Singapore: World Scientific), pp. 144–169.

Mayer, U., Torres Ruiz, R.A., Berleth, T., Miséra, S., and Jürgens, G. (1991). Mutations affecting body organization in the *Arabidopsis* embryo. Nature *353*, 402–407.

Mayer, U., Büttner, G., and Jürgens, G. (1993). Apical-basal pattern formation in the *Arabidopsis* embryo: studies on the role of the gnom gene. Development *117*, 149–162.

McIntosh, K., Pickett-Heaps, J.D., and Gunning, B.E.S. (1995). Cytokinesis in *Spirogyra*: integration of cleavage and cell-plate formation. Int. J. Plant Sci. *156*, 1–8.

Miséra, S., Müller, A.J., Weiland-Heidecker, U., and Jürgens, G.

(1994). The *FUSCA* genes of *Arabidopsis*: negative regulators of light responses. Mol. Gen. Genet. *244*, 242–252.

Neufeld, T.P., and Rubin, G.M. (1994). The Drosophila *peanut* gene is required for cytokinesis and encodes a protein similar to yeast putative bud neck filament proteins. Cell *77*, 371–379.

Olszewski, N.E., Martin, F.B., and Ausubel, F.M. (1988). Specialized binary vector for plant transformation: expression of the *Arabidopsis thaliana AHAS* gene in *Nicotiana tabacum*. Nucl. Acids Res. *16*, 10765–10782.

Owen, H.A., and Makaroff, C.A. (1995). Ultrastructure of microsporogenesis and microgametogenesis in *Arabidopsis thaliana* (L.) Heynh. ecotype Wassilewskija (Brassicaceae). Protoplasma *185*, 7–21.

Pelham, H.R.B. (1993). Is epimorphin involved in vesicular transport? Cell *73*, 425–428.

Preston, R.A., Manolson, M.F., Becherer, K., Weidenhammer, E., Kirkpatrick, D., Wright, R., and Jones, E. (1991). Isolation and characterization of *PEP3*, a gene required for vacuolar biogenesis in *Saccharomyces cerevisiae*. Mol. Cell. Biol. *11*, 5801–5812.

Rogers, S.O., and Bendich, A.J. (1988). Extraction of DNA from plant tissue. In Plant Molecular Biology Manual A6 (Dordrecht, The Netherlands: Kluwer Academic Publishers), pp. 1–10.

Röper, W., and Röper, S. (1977). Centripetal wall formation in roots of *Vicia faba* after caffeine treatment. Protoplasma *93*, 89–100.

Sambrook, J., Fritsch, E.F., and Maniatis, T. (1989). Molecular Cloning: A Laboratory Manual (Cold Spring Harbor, New York: Cold Spring Harbor Press).

Scheres, B., Di Laurenzio, L., Willemsen, V., Hauser, M.-T., Janmaat, K., Weisbeek, P., and Benfy, P.N. (1995). Mutations affecting the radial organization of the *Arabidopsis* root display specific defects throughout the embryonic axis. Development *121*, 53–62.

Schulze, K.L., Broadie, K., Perin, M.S., and Bellen, H.J. (1995). Genetic and electrophysiological studies of Drosophila syntaxin-1A demonstrate its role in nonneuronal secretion and neurotransmission. Cell *80*, 311–320.

Shevell, D.E., Leu, W.-M., Gilimor, C.S., Xia, G., Feldmann, K.A., and Chua, N.-H. (1994). *EMB30* is essential for normal cell division, cell expansion, and cell adhesion in Arabidopsis and encodes a protein that has similarity to Sec7. Cell *77*, 1051–1062.

Simanis, V. (1995). The control of septum formation and cytokinesis in fission yeast. Semin. Cell Biol. *6*, 79–87.

Spring, J., Kato, M., and Bernfield, M. (1993). Epimorphin is related to a new class of neuronal and yeast vesicle targeting proteins. Trends Biochem. Sci *18*, 124–125.

Südhof, T. (1995). The synaptic vesicle cycle: a cascade of protein-protein interactions. Nature *375*, 645–653.

Swofford, D.L. (1993). PAUP: Phylogenetic Analysis Using Parsimony, Version 3.1 (Champaign, Illinois: Illinois Natural History Survey).

Timberlake, W.E. (1986). Isolation of stage-specific genes from fungi. In Biology and Molecular Biology of Plant Pathogens, J. Bailey, ed. (Berlin: Springer), pp. 343–357.

Torres Ruiz, R.A., and Jürgens, G. (1994). Mutations in the *FASS* gene uncouple pattern formation and morphogenesis in *Arabidopsis* development. Development *120*, 2967–2978.

Trezzini, G.F., Horrichs, A., and Somssich, I.E. (1993). Isolation of putative defense-related genes from *Arabidopsis thaliana* and expression in fungal elicitor-treated cells. Plant Mol. Biol. *21*, 385–389.

Weigel, D., Alvarez, J., Smyth, D.R., Yanofsky, M.F., and Meyerowitz, E.M. (1992). *LEAFY* controls floral meristem identity in Arabidopsis. Cell *69*, 843–859.

Whitelam, G., Johnson, E., Peng, J., Carol, P., Anderson, M.L., Cowl, J.S., and Harberd, N.P. (1993). Phytochrome A null mutants of *Arabidopsis* display a wild-type phenotype in white light. Plant Cell *5*, 757–768.

Wick, S.M. (1991). Spatial aspects of cytokinesis in plant cells. Curr. Opin. Cell Biol. *3*, 253–260.

GenBank Accession Numbers

The accession numbers for the sequences reported in this paper are U39451 and U39452.